

Original Article

Open Access



# A sequential deposition of amyloid beta oligomers, plaques and phosphorylated tau occurs throughout life in the canine retina

Umma Habiba<sup>1</sup>, John Morley<sup>1</sup>, Mark Krockenberger<sup>2</sup>, Brian A. Summers<sup>3</sup>, Mourad Tayebi<sup>1</sup>

<sup>1</sup>School of Medicine, Western Sydney University, Campbelltown, NSW 2560, Australia.

<sup>2</sup>Faculty of Science, University of Sydney, Camperdown, NSW 2050, Australia.

<sup>3</sup>School of Veterinary Medicine, Melbourne University, Victoria, Werribee 3030, Australia.

**Correspondence to:** Dr. Mourad Tayebi, School of Medicine, Western Sydney University, Campbelltown, NSW 2560, Australia.  
E-mail: m.tayebi@westernsydney.edu.au

**How to cite this article:** Habiba U, Morley J, Krockenberger M, Summers BA, Tayebi M. A sequential deposition of amyloid beta oligomers, plaques and phosphorylated tau occurs throughout life in the canine retina. *Ageing Neur Dis* 2022;2:7. <https://dx.doi.org/10.20517/and.2022.06>

**Received:** 25 Feb 2022 **First Decision:** 21 Mar 2022 **Revised:** 25 Apr 2022 **Accepted:** 18 May 2022 **Published:** 25 May 2022

**Academic Editor:** Weidong Le **Copy Editor:** Peng-Juan Wen **Production Editor:** Peng-Juan Wen

## Abstract

**Aims:** Cerebral amyloid burdens may be found in otherwise cognitively intact adults, often not showing worsening deficits with passing years. Alzheimer's transgenic rodents have been widely used to investigate this phenomenon, but a spontaneous disorder in other animals, such as dogs that cohabit with humans and thus may have some shared environmental risks, may contribute and offer opportunities not possible in the smaller laboratory animals. In animals, the spontaneous disorder most comparable to Alzheimer's disease (AD) affects mature to aged dogs and is designated canine cognitive dysfunction. Motivated by AD, many studies have revealed that amyloid progressively accumulates in the canine central nervous system, including the retina. Here, we investigated whether deposits of amyloid and/or tau can be found in the canine retina of neurologically normal animals from the first year of life to the elderly. Suppose canine ocular amyloid and tau are present from early life. In that case, that raises the question of whether similar patterns of accumulation occur in man, whether as part of aging, AD, or other.

**Methods:** This study used eye tissues from 30 dogs with a variety of ophthalmic or other orbital disorders, of which 7/30 were 1-2 years old. Tissues were subdivided into dogs of three different age groups: young (1-5 years old),



© The Author(s) 2022. **Open Access** This article is licensed under a Creative Commons Attribution 4.0 International License (<https://creativecommons.org/licenses/by/4.0/>), which permits unrestricted use, sharing, adaptation, distribution and reproduction in any medium or format, for any purpose, even commercially, as long as you give appropriate credit to the original author(s) and the source, provide a link to the Creative Commons license, and indicate if changes were made.



middle (6-10 years old), and old ( $\geq 11$  years old).

**Results:** Following immunostaining of tissue sections with nanobodies against retinal  $A\beta_{1-40}$  and  $A\beta_{1-42}$  oligomers, and antibodies against  $A\beta$  plaques ( $A\beta p$ ) and hyperphosphorylated Tau (p-Tau), our investigations revealed that accumulation of  $A\beta_{1-40}$  and  $A\beta_{1-42}$  oligomers were widespread in the retina in all age groups. In contrast,  $A\beta p$  were detected in the middle and old age groups but not in the young age group. Furthermore, p-Tau staining was observed in four old dogs only, while other dogs were p-Tau free. Interestingly, both  $A\beta o$  and  $A\beta p$  co-localized in the middle and old age groups of dogs. Moreover, diffuse granular p-Tau co-localized with intracellular  $A\beta o$  in the old age group. Finally, we also observed co-localization of  $A\beta o$  and  $A\beta p$  in the retinal vasculature which might be similar to cerebral amyloid angiopathy associated with AD.

**Conclusion:** As far as we know, the presence of amyloid and tau in the canine retina is hitherto unreported. If similar, early-in-life subclinical retinal deposits occur in a human cohort perhaps identified by AD genetic risk factors, following this group may offer the prospect of preclinical therapeutic intervention in imminent dementia, a strategy recognized as likely necessary to impact this burgeoning disorder.

**Keywords:** Alzheimer's disease, canine cognitive dysfunction, retina, early diagnosis,  $A\beta o$ ,  $A\beta p$ , p-Tau

## INTRODUCTION

The principal neuropathological lesions in Alzheimer's disease (AD) brains include extracellular neuritic and/or diffuse plaques containing amyloid-beta ( $A\beta$ ), intracellular tau protein (p-Tau) in the form of neurofibrillary tangles (NFTs) in addition to cerebral amyloid angiopathy (CAA), ubiquitin, severe synaptic loss, neuronal death, and brain atrophy<sup>[1-4]</sup>. While the deposition of  $A\beta$  in the human brain has traditionally been accepted as a major hallmark of AD<sup>[5]</sup>, its accumulation is also observed in about 20% of cognitively unimpaired, aged individuals<sup>[6,7]</sup>. For decades, the association of  $A\beta$  with AD has been demonstrated, but the significance and impact of  $A\beta$  accumulation in healthy individuals are both poorly understood<sup>[8]</sup> and a source of confusion. For example, previous studies did not establish a clear correlation with memory loss in the aging brain<sup>[9-11]</sup>. Previous reports documented the progressive accumulation of both  $A\beta$  plaques ( $A\beta p$ ) in the brain<sup>[12,13]</sup> and  $A\beta$  oligomers ( $A\beta o$ ) in the brain and periphery of cognitively unimpaired individuals<sup>[14,15]</sup>. A study by Lesne *et al.* measured the levels of three  $A\beta o$  "species", including  $A\beta$  trimers,  $A\beta^*56$  and  $A\beta$  dimers, in brain tissues from 75 cognitively unimpaired individuals, including young children and adolescents<sup>[14]</sup>. The authors showed that  $A\beta$  trimers were present in the central nervous system (CNS) of children and adolescents, and their levels increased progressively with age, suggesting that this particular  $A\beta o$  could be used to track the potential progression into AD from a very young age. Another study investigated the relationship between amyloid levels and memory performance<sup>[15]</sup>. This study, which included 147 participants divided into three groups of adults 30-49, 50-69, and 70-89 years of age, established a clear relationship between episodic memory performance and amyloid accumulation in the youngest group<sup>[15]</sup>. A longitudinal study by Hanseuw *et al.* demonstrated a correlation between  $A\beta/p$ -Tau and declining cognition in 60 clinically normal individuals aged between 65-85 years<sup>[16]</sup>. The authors concluded that there was a positive correlation between  $A\beta/p$ -Tau positron emission tomography (PET) and cognition, where participants with high  $A\beta$  and tau were at higher risk of developing mild cognitive impairment (MCI)<sup>[16]</sup>. These studies highlighted the importance of investigating and characterizing normal aging in cognitively unimpaired younger individuals to identify those at risk of progressive increase of AD-associated neuropathology changes and cognitive impairment and establish a time frame for early diagnostic and therapeutic intervention. However, such studies are difficult to implement in human subjects and will take decades to deliver any meaningful outcome<sup>[8,17]</sup>.

Currently available transgenic animal models of AD do not replicate the subtle clinical and pathological features of the disease, as demonstrated by their lack of reproducible therapeutic outcomes<sup>[18,19]</sup>. As the dog's age, there is an anatomically defined accumulation of A $\beta$  peptides in the CNS, while less is known about cerebral p-Tau deposition. Some animals will develop a progressive cognitive decline with loss of learned behaviors and memory, a syndrome named canine cognitive dysfunction (CCD)<sup>[20-24]</sup>, with CNS changes similar to the neuropathological hallmarks characteristic of AD<sup>[25-28]</sup>. In those destined to develop AD, amyloid precursor protein (APP) is sequentially cleaved by  $\beta$  and  $\gamma$  secretase leading to the production of A $\beta$  peptide fragments (36-43 amino acids), which then aggregate and deposit as plaques<sup>[4,5,29]</sup>. The canine APP and A $\beta$  peptides are 98% and 100% identical to their human counterparts<sup>[24]</sup>. In older dogs and others affected with CCD, A $\beta$  deposits as diffuse plaques, while the dense core of humans' mature plaques is very rare or absent<sup>[20,21,27,30]</sup>.

There are two major isoforms of A $\beta$ , A $\beta_{1-40}$  (~80%-90%) and A $\beta_{1-42}$  (~5%-10%) and three major assemblies<sup>[31-34]</sup> recognized in man and animals/dogs, including monomeric A $\beta$ , A $\beta$ o containing 12-24 monomers which become elongated to form protofibrils and finally insoluble fibrils<sup>[35]</sup>. Among these three stages, A $\beta$ o is thought to be the most toxic to neurons and responsible for the structural and functional pathologic changes associated with AD<sup>[36-39]</sup>. Likewise, a previous study reported that cognitive decline occurs before the accumulation of A $\beta$ p in CCD, supporting the premise that earlier assembly states of A $\beta$  may be the toxic species<sup>[23]</sup>. In addition, CAA, ubiquitin, and severe synaptic loss have also been reported in CCD<sup>[20,40-43]</sup>. Another cardinal pathological hallmark of AD is the accumulation of p-Tau<sup>[3,4]</sup>. Several phosphorylation sites were identified on tau in aged dogs including Thr181<sup>[42]</sup>, Ser422<sup>[43]</sup>, Ser202/Thr205<sup>[40,43]</sup>, Ser396<sup>[30,40,43]</sup>, Ser189, and Ser207<sup>[44]</sup>; however, demonstrating the presence of NFTs has been infrequent compared to the consistent demonstration of amyloid oligomers and diffuse plaques. A study by Schmidt and colleagues using anti-pT205, AT8, AT100, PHF-1, and anti-pT422 antibodies seeking the presence of tau pathology in 24 dogs aged between two and nineteen years, showed that three 13-15-year-old dogs displayed p-Tau and only one 15-year-old Pekingese dog displayed NFT-like appearance<sup>[43]</sup>.

In AD, visual disturbances are one of the early complaints and include loss of color vision, impairment of peripheral vision and object recognition, contrast sensitivity, and decreased visual memory and perception<sup>[45-47]</sup>. A recent longitudinal study of 1349 older adults showed that poor visual acuity paralleled the development of dementia<sup>[48]</sup>, suggesting the possibility that ocular disturbances can be used as an early predictor of dementia risk in the older population<sup>[48]</sup>. Moreover, post-mortem studies of AD and animal models of AD demonstrated a strong association between retinal accumulation of A $\beta$ o<sup>[49,50]</sup>. A $\beta$  plaques<sup>[51,52]</sup>, p-Tau<sup>[53,54]</sup> and brain depositions and cognitive decline, where retinal A $\beta$ o was shown to deposit earlier than the brain and before deficits in cognition. Although, to our knowledge, age-dependent retinal deposition of A $\beta$ o and/or A $\beta$ p has not been investigated in AD and cognitively unimpaired individuals, including children and adolescents, our recent studies in AD mice models confirmed the conversion of cerebral and retinal A $\beta$ o to A $\beta$ p in an age-dependent manner, where retinal A $\beta$ o was detected as early as 3-month old APP/PS1 mice, before brain pathology and cognitive decline were observed<sup>[49,55]</sup>.

In this study, we investigated the retinal accumulation of A $\beta$ o, A $\beta$ p, and p-Tau in three age groups of genetically diverse and neurologically intact populations of dogs. Here, following immunohistochemistry and immunofluorescence analysis, we confirmed the presence of retinal A $\beta_{40}$  and A $\beta_{42}$  oligomers, A $\beta$ p, and p-Tau. Retinal A $\beta_{40}$  and A $\beta_{42}$  oligomers deposition was conspicuous and widespread and observed in all age groups, including the young 1-5-year-old neurologically intact group. Moreover, retinal co-localization of A $\beta_{40}$ /A $\beta_{42}$  oligomers and A $\beta$ p was observed in few middle-aged dogs and most dogs in the old neurologically intact age group, while retinal co-localization of A $\beta_{40}$ /A $\beta_{42}$  oligomers and p-Tau was only seen in the old

neurologically intact age group of dogs. Morphologically, extracellular A $\beta$ p deposits appeared as small, dot-like rounded deposits, while intracellular p-Tau deposits adopted a diffuse appearance in the retinal layers<sup>[54]</sup>. No NFTs or neuropil threads were observed in these dogs. Taken together, these results highlight the importance of further investigations of AD-related pathology in the retina of presymptomatic children and adolescents to gain insight into disease progression and potentially identify early at-risk individuals to help implement speedy therapeutic interventions.

## METHODS

### Dog eye samples and animal ethics

Sections of eyes used in this study were prepared from archived cases in the Comparative Ocular Pathology Laboratory of Wisconsin (COPLOW) at the Department of Pathobiological Sciences, School of Veterinary Medicine, University of Wisconsin, Madison. Surgical enucleations had been submitted by practicing veterinarians to COPLOW for routine pathological diagnosis. These canine eyes came from 30 random, genetically diverse dogs (15 different breeds) ranging from 1 to 16 years of age with a broad variety of ocular disorders [Tables 1 and 2]. Such tissues, historically submitted for disease investigation purposes, are not subject to approval by institutional animal ethical regulations.

### Tissue preparation

Enucleated eyes were submitted to the laboratory fixed in 10% neutral buffered formalin. On receipt, they were examined for gross abnormalities before trimming, followed by processing overnight using a Leica ASP300S tissue processor (Leica biosystem, Wetzlar, Germany). Tissues were then embedded in paraffin blocks and sectioned at 4 $\mu$ m thickness using a Leica RM2235 microtome (Leica biosystem, Wetzlar, Germany) and placed on charged slides. Sections were then stained with hematoxylin and eosin (H&E) and Congo red (CR). Further sections were used for immunohistochemistry (IHC) and immunofluorescence (IF) staining, and both upper and lower parts of the retina were assessed.

### Hematoxylin and eosin staining

Paraffin sections were dewaxed by two changes of absolute xylene for 5 min each. Sections were rehydrated using two changes of 100% ethanol for 2 min each, 95% ethanol for 3 min, 70% ethanol for 2 min, and finally rinsed in deionized water for 2 min. H&E stain was then performed by adding Gill II Haematoxylin solution (Leica Biosystems, Wetzlar, Germany), followed by 1% acid alcohol and subsequently eosin stain (Leica Biosystems, Wetzlar, Germany). Finally, the sections were dehydrated with increasing concentrations of ethanol, from 70%, 95% to 100%, then dewaxed by two changes of xylene and finally mounted with xylene-based mounting media (Sigma Aldrich, Missouri, United States)<sup>[56]</sup>. H&E staining was used to assess retinal morphology, the neuronal population within the eye.

### Congo red staining

Initially, the CR working solution was prepared by mixing 50 ml Congo red solution and 0.5 ml potassium hydroxide solution supplied in the Congo red amyloid special stain kit (Leica Biosystems, Wetzlar, Germany). Retinal sections were placed in the working solution for 20 min and then rinsed in 5-8 changes of deionized water. This was followed by staining with Gill II Haematoxylin (Leica Biosystems, Wetzlar, Germany) for 1-3 min and rinsing in 3 changes of deionized water. Sections were then dehydrated in two changes of 95% alcohol followed by three changes of absolute alcohol for one minute each. Finally, the sections were cleared in two changes of xylene and mounted in a xylene miscible medium. Amyloid fibrils appeared as dull to red brick under light microscopy (Olympus CX 43, Shinjuku, Tokyo, Japan) and apple green birefringent under polarized light (Olympus CX 43, Shinjuku, Tokyo, Japan).

**Table 1. Signalment for 30 dogs and their retinal A $\beta$  oligomers and plaques IHC scores**

Age groups	Age (year)	Sex	Breed	Size	Pathological A $\beta$ IHC findings in the dog retina	
					A11 - A $\beta$ oligomers	4G8 - A $\beta$ plaques
Young (1-5 years)	1	SF	Staffordshire terrier	Medium	+	-
	1.4	M	Siberian husky	Medium	-	-
	1.8	SF	Mixed breed	ND*	+++	-
	1.10	SF	Siberian husky	Medium	++	-
	2	F	Chihuahua mix	Toy	+++	-
	2	M	Bichon frise mix	Small	+	-
	2	NM	Shih Tzu	Small	+	-
	3	NM	German shepherd	Large	+++	-
	3	F	Giant schnauzer	Large	+	-
Middle age (6-10 years)	3.6	M	Siberian husky	Medium	+	-
	7	NM	Hound mixed	Medium	-	-
	8	SF	Bedlington terrier	Small	-	-
	8	SF	Cocker spaniel	Medium	-	-
	8	M	Mixed breed	ND*	-	-
	8	M	Cocker spaniel	Medium	+	-
	8	F	German shepherd mix	Large	-	-
	8	SF	Great dane dog	Giant	-	-
	9	M	Jack Russell terrier dog	Small	-	-
Elderly (11-16 years)	9.5	SF	Boxer dog	Large	-	-
	9.9	SF	Cocker spaniel	Medium	-	-
	11	NM	Mixed breed	ND*	-	-
	11	NM	Beagle	Small	-	-
	11.9	SF	Bouvier des flanders	Large	+	-
	12	SF	German shepherd	Large	-	++
	12	SF	German shepherd mix	Large	-	-
	12	NM	Husky mix	Medium	-	-
	12.8	NM	Shih-tzu	Small	-	++
13	NM	Border collie	Medium	-	-	
15	SF	Basset hound	Medium	-	+	
16	SF	Shih Tzu	Small	-	-	

Sizes were determined according to the American Kennel Club (AKC)<sup>[76]</sup>. Size range between 34 -  $\geq$  54 kg is considered "giant", 24-38 kg is considered "large", 15-29 kg is considered "medium", 3-15 kg is considered "small", and 0.9-4 kg is considered "toy". A $\beta$  oligomers and A $\beta$  plaques staining intensity were semi-quantitatively analyzed and scored across the retinal layers under the brightfield microscope (Olympus CX 43, Shinjuku, Tokyo, Japan). The total area was examined at 40 magnification and categorized into no immunostaining "-"; low immunoreactivity found only in limited areas of the retinal layers "+", moderate immunoreactivity where A $\beta$  deposits were more apparent "++"; and finally strong immunoreactivity with widespread A11 and 4G8 positive A $\beta$  labeling were exhibited "+++". ND\*: Not determined; SF: spayed female; F: female; NM: neutered male; M: male; IHC: immunohistochemical.

### Immunohistochemical staining of amyloid-beta plaques and amyloid-beta oligomers

Eye sections that contained the retina were pre-treated using the 2100 antigen retriever (Aptum Biologics Ltd, Southampton, United Kingdom) to expose the target epitopes. The sections were then treated with 90% formic acid for 5 min at room temperature (RT) followed by cell membrane permeabilization, achieved by using 0.1% Triton X for 1 min before the addition of 0.3% H<sub>2</sub>O<sub>2</sub> for 15 min to inactivate endogenous peroxidases. Sections were then blocked with protein block serum-free (Agilent, City, Country) for 15 min. The sections were then stained for 1 h with the following primary antibodies in phosphate-buffered saline (PBS): mouse purified 4G8 anti-A $\beta$ <sub>17-24</sub> (1:500; Bio legend, San Diego, CA, USA) or A11 rabbit anti-A $\beta$ o (1:250; Merck Millipore, Burlington, MA, USA) antibodies. After washing with PBS, sections were

**Table 2. Signalment for 30 dogs, their ophthalmological disorders, and retinal A $\beta$  and p-Tau IF scores**

Age groups	Age (year)	Sex	Breed	Size	Ophthalmological disorders which resulted in enucleation	Pathological IF findings in the dog retina			
						A $\beta$ <sub>40</sub> oligomers	A $\beta$ <sub>42</sub> oligomers	A $\beta$	p-Tau
Young (1-5 years)	1	SF	Staffordshire terrier	Medium	Anterior segment dysgenesis	+	+	-	-
	1.4	M	Siberian husky	Medium	Anterior segment dysgenesis	-	-	-	-
	1.8	SF	Mixed breed	ND*	Anterior segment dysgenesis	+++	+++	-	-
	1.10	SF	Siberian husky	Medium	Anterior segment dysgenesis	+++	+++	-	-
	2	F	Chihuahua mix	Toy	Anterior segment dysgenesis	+++	+++	-	-
	2	M	Bichon frise mix	Small	Proptosis	+++	+++	-	-
	2	NM	Shih Tzu	Small	Melanoma limbal	++	++	-	-
	3	NM	German shepherd	Large	Rhabdomyosarcoma orbital	+++	+++	-	-
	3	F	Giant schnauzer	Large	Phthisis bulbi	++	++	-	-
	3.6	M	Siberian husky	Medium	Anterior segment dysgenesis	++	++	-	-
Middle age (6-10 years)	7	NM	Hound mixed	Medium	Hemangiosarcoma	-	-	-	-
	8	SF	Bedlington terrier	Small	Neoplasia	-	-	-	-
	8	SF	Cocker spaniel	Medium	Conjunctivitis	+++	+++	+	-
	8	M	Mixed breed	ND*	Conjunctival melanoma	+++	+++	+	-
	8	M	Cocker spaniel	Medium	Pre glaucoma	+++	+++	+++	-
	8	F	German shepherd mix	Large	Mast cell tumor	++	++	+	-
	8	SF	Great dane dog	Giant	Complex apocrine adenocarcinoma	+	+	-	-
	9	M	Jack Russell terrier dog	Small	Sialoadenitis	++	++	-	-
	9.5	SF	Boxer dog	Large	Hemangioma	+	+	-	-
	9.9	SF	Cocker spaniel	Medium	Adenocarcinoma a orbital	+++	+++	+++	-
Elderly (11-16 years)	11	NM	Mixed breed	ND*	Squamous cell carcinoma	-	-	-	-
	11	NM	Beagle	Small	Melanoma conjunctival	+++	+++	+++	-
	11.9	SF	Bouvier des flanders	Large	Melanoma eyelid	+	+	-	-
	12	SF	German shepherd	Large	Melanoma eyelid	+++	+++	+++	+++
	12	SF	German shepherd mix	Large	Melanoma conjunctival	+++	+++	+++	-
	12	NM	Husky mix	Medium	Orbital carcinoma	+++	+++	++	+++
	12.8	NM	Shih-tzu	Small	Glaucoma	+++	+++	++	+++
	13	NM	Border collie	Medium	Melanoma skin	+++	+++	+++	+++
15	SF	Basset hound	Medium	Conjunctival hemangiosarcoma	+++	+++	+++	-	
16	SF	Shih Tzu	Small	Squamous cell carcinoma	+	+	-	-	

Existing ophthalmological conditions of the 30 neurologically intact unimpaired dogs were determined from the clinical report. Sizes were determined according to the American Kennel Club (AKC). Size range between 34 -  $\geq$  54 kg is considered "giant", 24-38 kg is considered "large", 15-29 kg is considered "medium", 3-15 kg is considered "small", and 0.9-4 kg is considered "toy". A $\beta$  oligomers A $\beta$  plaques and p-Tau staining intensity were semi-quantitatively analyzed and scored across the retinal layers under the confocal microscope (LSM800, Zeiss, Oberkochen, Germany). The total area was examined at 40 magnification and categorized into no immunostaining "-"; low immunoreactivity found only in limited areas of the retinal layers "+", moderate immunoreactivity where deposits were more apparent "++"; and finally strong immunoreactivity with widespread A $\beta$ , A $\beta$ , and p-Tau labeling was exhibited "+++". ND\*: Not determined; SF: spayed female; F: Female; NM: neutered male; M: male; IF: immunofluorescence.

incubated for 1 h at RT with the following secondary antibodies in PBS: HRP-conjugated anti-mouse IgG (Sigma-Aldrich, Missouri, United States) or anti-rabbit IgG (Sigma-Aldrich, Missouri, United States). The

sections were then washed three times with PBS before the addition of the 3,3'-Diaminobenzidine substrate chromogen system and incubated for 5-10 min. The sections were then counterstained with hematoxylin for 1 min before mounting. Sections were finally imaged using Olympus CX 43 light microscopy (Shinjuku, Tokyo, Japan).

The staining intensity was semi-quantitatively analyzed and scored across the retinal layers. Each bright field was examined at 40× magnification and categorized into no immunostaining “-”; low immunoreactivity, found in limited areas of the retinal layers “+”; moderate immunoreactivity where A $\beta$  deposits were numerous “++”; and finally strong immunoreactivity with widespread A11 and 4G8 positive A $\beta$  labeling “+++” [Table 1].

### Immunofluorescence detection and co-localization studies

To investigate whether A $\beta$  co-localized with A $\beta$ p or with p-Tau, we performed immunofluorescence double labeling using camelid-derived single domain anti-A $_{40}$  (PRIOAD12) or anti-A $_{42}$  (PRIOAD13) oligomer antibodies with 4G8 anti-A $\beta$ p antibody (Bio legend, San Diego, California, United States) or anti-phosphorylated tau AT8 antibody targeting amino acid residues Ser202/Thr205 (Thermo-fisher Scientific, Massachusetts, United States). Slides were processed as described above for IHC before adding the primary antibodies. The sections were double-stained with either PRIOAD 12 (1:500) or PRIOAD 13 (1:500)<sup>[57]</sup> and 4G8 antibody overnight (1:500) or AT8 (1:500) and either PRIOAD 12 (1:500) or PRIOAD 13 (1:500). Sections were then washed in Tris-buffered saline with 0.05% Tween 20 (TBST) and incubated with secondary antibodies at a dilution of 1:500, including goat anti-llama IgG conjugated to FITC (Bethyl Laboratories, Inc, Texas, USA) or donkey-anti-mouse IgG conjugated to Texas red (Sigma-Aldrich, Missouri, United States) for 2 hours at room temperature. Other sections were used as negative control and stained with secondary antibodies with the omission of the primary antibodies. Retinal sections derived from an APP/PS1 and TAU58/2 transgenic mice models<sup>[58,59]</sup> were used as positive control and stained with anti-A $\beta$  and anti-P-Tau antibodies, respectively. The sections were covered, slipped with paramount aqueous mounting medium (Dako, Agilent, Santa Clara, California, United States), sealed, and dried overnight. Finally, the sections were visualized with LSM800 confocal microscope with a standard FITC/Texas Red double band-pass filter set (Zeiss, Oberkochen, Germany).

## RESULTS

### Histological assessment of the retina in 30 dogs

We performed H&E staining of the canine eye sections and examined the retinal layers to assess their general morphological appearance and identify pathological changes such as vacuolation, neuronal death, and eosinophilic deposits<sup>[49,55]</sup>. No specific lesions were observed in the retinal layers of the young and middle age groups (data not shown). However, scattered eosinophilic deposits in the ganglion cell layer (GCL) and inner nuclear layer (INL) of the retina were noticeable in 5/10 dogs in the older age group (11-16 years old), including an 11-year-old Beagle, a 12-year-old German shepherd, a 12-year-old Husky mix, a 12.8-year-old Shih Tzu, and a 15-year-old Basset hound [Figure 1A and B]. Furthermore, CR staining used to detect any amyloid fibrils and CAA in eye sections of the dogs did not display any staining in the retina tissues from all age groups (data not shown).

### Immunohistochemical detection of A $\beta$ oligomers and plaques in the retina of 30 dogs

While demonstrated in the CNS of aged animals including cats and bears<sup>[24,60]</sup>, dogs have been more comprehensively studied and shown to develop human type A $\beta$  deposition at a very young age. Retinal tissues stained with A11 exhibited intracellular A $\beta$ o depositions in the outer nuclear layer (ONL), INL, and GCL [Figure 1C and D]. The intraneuronal A $\beta$ o intensity following A11 staining ranged from low (+), moderate (++) to strong (+++) in all dogs in the young age group except a 1.4 years old male Siberian husky

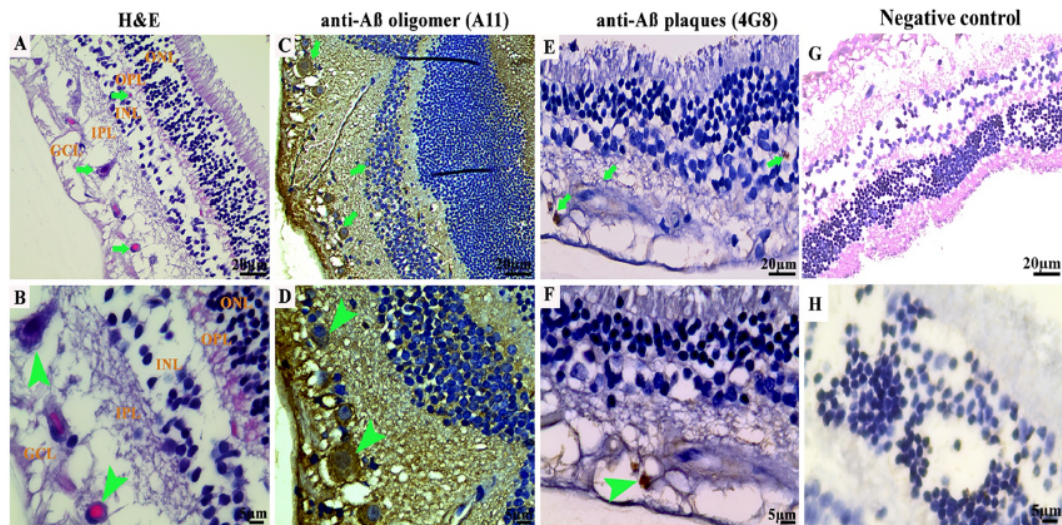


**Figure 1.** Photomicrographs of the microscopic lesions in the canine retina. The retina in a 12-year-old German shepherd dog. Eosinophilic deposits (green arrows) were observed in the ganglion cell layer (GCL) and inner nuclear layer (INL). Representative of 10 cases of old-aged dogs. Hematoxylin and eosin (H&E) 40 $\times$ . (B) Higher magnification of the deposits in image (A) (green arrowhead) in the GCL. H&E 100 $\times$ . (C) Retina of a 3-year-old German shepherd dog. Immunohistochemical staining with A11 anti-A $\beta$ o IgG antibody exhibited cytoplasmic A $\beta$ o depositions in the GCL and INL (green arrows). Representative of 10 cases of young age group. IHC 40 $\times$ . (D) Higher magnification of deposits from image (C) in the GCL (green arrowheads). IHC 100 $\times$ . (E) Retina of a 12-year-old German shepherd mix dog. Immunohistochemical staining with 4G8 anti-A $\beta$ p IgG antibody exhibited extracellular A $\beta$  aggregates in the GCL and INL (green arrows). IHC 40 $\times$ . (F) Higher magnification of deposit from image (E) in the GCL (green arrowhead). (G and H) Representative retinal sections derived from dogs of all age groups stained with secondary antibodies with the omission of the primary antibody did not show any depositions (40 $\times$  and 100 $\times$ , respectively). The photomicrographs were taken from the peripheral region of the retina - away from the optic disc. Representative of all 30 dogs examined. IHC 100 $\times$ . IHC: Immunohistochemistry.

that did not display any A11 positive stain [Supplementary Figure 1A]. Of note, retinal sections derived from wild-type mice were used as negative control following immunofluorescence staining [Supplementary Figure 1B and C].

A spayed female mixed breed aged 1.8 years, a female Chihuahua aged 2 years, and a neutered male German shepherd aged 3 years showed strong (+++) accumulation of A11 positive A $\beta$ o [Figure 1C and D]. Two dogs displayed a low amount (+) of A11 positive A $\beta$ o in the retinal layers in the middle and old age groups, including an 8-year-old male Cocker spaniel and an 11.9-year-old spayed female Bouvier des Flanders [Table 1]. In addition, 4G8-positive small rounded and dot-like extracellular A $\beta$ p deposits were observed in the INL, inner plexiform layer (IPL), and GCL [Figure 1E and F] of the retina. They were structurally different from the typical large diffuse plaques normally observed in dog brains with CCD<sup>[21,30,61]</sup>. The extracellular A $\beta$ p intensity following 4G8 staining ranged from low (+) to moderate (++) in some dogs in the old age group, including a 15-year-old spayed female Basset hound, a 12.8-year-old neutered male Shih Tzu, and a 12-year-old spayed female German shepherd. Other dogs in this age group were all negative for 4G8 staining [Table 1, Figure 1E and F]. Representative retinal sections derived from dogs of all age groups stained with secondary antibodies with the omission of the primary antibody did not show any depositions [Figure 1G and H].

#### Immunofluorescence detection and co-localization of retinal A $\beta$ <sub>40</sub>, A $\beta$ <sub>42</sub> oligomers, and A $\beta$ plaques in the retina of 30 dogs

To confirm the presence of retinal A $\beta$ <sub>40</sub> and A $\beta$ <sub>42</sub> oligomers and to determine whether A $\beta$ <sub>40</sub> and/or A $\beta$ <sub>42</sub> oligomers co-localized with A $\beta$ p in the retinas of different age groups and breeds of neurologically intact dogs, we performed immunofluorescence double staining using PRIOAD12 (A $\beta$ <sub>40</sub> oligomers), PRIOAD13

(A $\beta_{42}$  oligomers) camelid-derived single domain anti-A $\beta$  oligomer and 4G8 anti-A $\beta$ p antibodies. Morphologically, A $\beta$  appeared as globular and annular in shape<sup>[55,62]</sup> and deposited intracellularly in the ONL, INL, and GCL [Figures 2-4]. 4G8 positive A $\beta$  plaques appeared morphologically as dot-like and small rounded extracellular deposits<sup>[50,54]</sup> in the outer plexiform layer (OPL), IPL, and GCL [Figures 2-4]. We found that both A $\beta_{40}$  and A $\beta_{42}$  oligomers staining was widespread in the majority of the dogs in young [Table 2, Figure 2A and B], middle [Table 2, Figure 3A and B], and old age groups [Table 2, Figure 4A and B]

except four dogs including a 1.4-years-old male Siberian husky, a 7-years-old neutered male Hound mixed, an 8-years-old spayed female Bedlington terrier and an 11-years-old mixed breed. In comparison, A $\beta$ p was absent in young dogs [Table 2, Figure 2C and D], but its presence in the middle age group was moderate [Table 2, Figure 3D and E] and conspicuous in the old age group [Table 2, Figure 4D and E]. Therefore, no co-localization of A $\beta$  and A $\beta$ p was noticed in the retinal layers of the young age group [Figure 2E-H]. However, retinal A $\beta$ p was shown to co-localize with A $\beta_{40}$  or A $\beta_{42}$  in the GCL, IPL & INL of the middle [Figure 3G, H, J and K] and old [Figure 4G, H, J and K] neurologically intact age groups. Co-localization of A $\beta$  oligomers and 4G8 positive A $\beta$  plaques were also exhibited in the retinal vessel wall, where young dogs didn't exhibit any co-localization, the middle age group showed scarce co-localization [Figure 3I and L], and the older age group exhibited conspicuous co-localization in the vessel wall [Figure 4I and L]. In the middle age group, two Cocker spaniels aged 8 years male and 9.9 years female respectively exhibited widespread co-localization of A $\beta$  and A $\beta$ p, and in the old age group, a neutered male Beagle aged 11 years, two spayed female German shepherds aged 12 years, a neutered male Border collie aged 13 years, and a spayed female Basset hound aged 15 years displayed strong and widespread co-localization of A $\beta$  and A $\beta$ p. This co-localization study revealed an age-dependent distribution and co-accumulation of A $\beta$  and A $\beta$ p in the retina of the neurologically intact dogs. We found that the young dogs exhibited widespread accumulation of A $\beta_{40}$  and A $\beta_{42}$  oligomers without any plaque deposits; in the middle age group, A $\beta_{40}$  and A $\beta_{42}$  oligomers accumulation was less conspicuous and, in some cases, co-localized with A $\beta$ p; and at the old age group, there was widespread and strong co-localization of A $\beta$  and A $\beta$ p strongly distributed in most dogs [Supplementary Figures 2 and 3]. Representative retinal sections derived from dogs of all age groups stained with secondary antibodies with the omission of the primary antibody did not show any co-localization [Supplementary Figure 4A-F]. Retinal sections derived from an APP/PS1 mouse were used as positive control and confirmed the presence of A $\beta_{40}$  and A $\beta_{42}$  oligomers [Supplementary Figure 5A and B] and A $\beta$ p [Supplementary Figure 5C]<sup>[49,55]</sup>.

### **Immunofluorescence co-localization of retinal A $\beta$ oligomers and phosphorylated tau in the retina of 30 dogs**

To confirm the presence of p-Tau and to investigate whether p-Tau co-localizes with A $\beta$ , we performed double fluorescence staining of A $\beta$  and p-Tau using PRIOAD 12 (A $\beta_{40}$ ) or PRIOAD 13 (A $\beta_{42}$ ) anti-oligomer<sup>[57]</sup> and AT8 anti-p-Tau antibody, targeting Ser202/Thr205<sup>[54]</sup>. A $\beta$  appeared as globular and annular in shape<sup>[55,62]</sup> [Figure 5A and B] and AT8 positive p-Tau appeared morphologically as diffuse and granular intracellular deposits<sup>[54]</sup> in the OPL, INL, IPL, and GCL [Figure 5C and D]. Overall, A $\beta$  and p-Tau did not display consistent co-localization in all age groups, as P-tau was only detected in the old age group and A $\beta_{40}$  or A $\beta_{42}$  oligomers were identified in all age groups. Among ten dogs in the old age group, only four dogs have displayed the presence of p-Tau including a spayed female German shepherd and a neutered male Husky aged 12 years, a neutered male Shih Tzu aged 12.8 years, and a neutered male Border collie aged 13 years, and they exhibited strong co-localization with A $\beta_{40}$  or A $\beta_{42}$  oligomers [Figure 5E-H]. Representative retinal sections derived from Tau 58/2 mouse were used as positive control and confirmed the presence of AT8 positive p-Tau [Supplementary Figure 5D]<sup>[58]</sup>. Representative retinal sections derived from dogs of all age groups stained with secondary antibodies with the omission of the primary antibody did not show any co-localization [Supplementary Figure 6A and B].

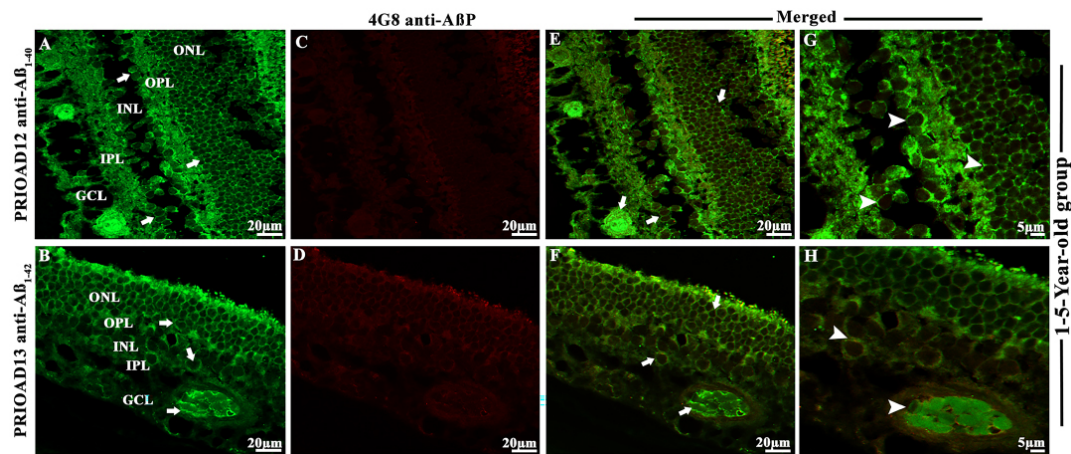


**Figure 2.** Immunofluorescence (IF) detection and co-localization of retinal amyloid-beta oligomers and amyloid-beta plaques in the dogs of the 1-5-year-old group. Retinal co-staining of oligomers with anti- $A\beta_{40}$  (PRIOAD12) or anti- $A\beta_{42}$  (PRIOAD 13) camelid-derived single domain antibodies (green) and plaques with anti- $A\beta$  (4G8) antibody (red) of a 3-year-old German shepherd dog (A-H). A and B show widespread accumulation of  $A\beta_{40}$  and  $A\beta_{42}$  oligomers in the GCL, INL, and ONL (white arrows) and retinal vasculature, respectively. IF 40 $\times$ . (C and D) No  $A\beta_p$  was detected in the retinal layers. IF 40 $\times$ . (E and F) Co-localization of  $A\beta_0$  and  $A\beta_p$  was not observed in the retinal layers of this animal ( $A\beta_0$  was present - white arrows). G and H are higher magnification 100 $\times$  of images (A and B) in the GCL and INL, ONL and retinal vasculature. Representative of 10 dogs in the younger age group (1-5 years). GCL: Ganglion cell layer; INL: inner nuclear layer; ONL: outer nuclear layer.

### Influence of demographic factors on the retinal deposition of $A\beta$ oligomers, $A\beta$ plaques, and phosphorylated tau in 30 dogs

To investigate the influence of the demographic factors on retinal  $A\beta$  and p-Tau deposition, staining intensity was compared with the age, breed, size, and sex of the neurologically intact dogs [Table 2].  $A\beta_{40}$  and  $A\beta_{42}$  oligomers,  $A\beta_p$  and p-Tau fluorescence intensity, were assessed at 40 $\times$  magnification. Immunoreactivity throughout the retinal layers was semi-quantified and categorized into no immunostaining “-”; low immunoreactivity, exhibited in limited areas of the retinal layers “+”; moderate immunoreactivity where deposits were more apparent “++” and finally strong immunoreactivity with widespread  $A\beta_0$ ,  $A\beta_p$  and p-Tau labeling “+++” [Table 2]. After comparing the age of the dogs and immunofluorescence staining scores, we found that both  $A\beta_{40}$  and  $A\beta_{42}$  oligomers staining was high in young dogs, which slightly decreased in the middle age group, then finally, an upward trend was noticed in older dogs [Table 2, Figure 6]. In comparison,  $A\beta_p$  was absent in young dogs, but its presence in the middle age group was moderate and high in the old age group [Table 2, Figure 6]. Finally, p-Tau deposits were not observed in the young and middle age groups, whereas old dogs exhibited widespread staining for p-Tau [Table 2, Figure 6]. However, when the size of the dog was compared with the pathological outcome, we found that six medium-sized dogs displayed strong  $A\beta_0$  staining and only two dogs exhibited strong p-Tau staining [Table 2, Figure 7]. In addition, seven dogs revealed strong  $A\beta_p$  staining, of which four were medium size [Table 2, Figure 7].

### Influence of eye pathology on the retinal deposition of $A\beta$ oligomers, $A\beta$ plaques, and phosphorylated tau in 30 dogs

Further, to understand whether the presence of pre-existing underlying eye pathology in the dogs may influence retinal  $A\beta$  and p-Tau depositions, we compared their staining intensity with the reported underlying clinical eye conditions [Table 2]. We found that four young dogs aged 1-5 years affected with anterior segment dysgenesis, a spectrum of disorders that affect the development of the anterior segment, including the cornea, iris, ciliary body, and lens<sup>[63-65]</sup>, displayed “moderate” to “strong” intensity staining for  $A\beta_{40}$  and  $A\beta_{42}$  oligomers [Table 2]. However, another two dogs in this age group and affected with anterior segment dysgenesis showed little to no deposition of  $A\beta_{40}$  and  $A\beta_{42}$  oligomers [Table 2]. Eighteen out of

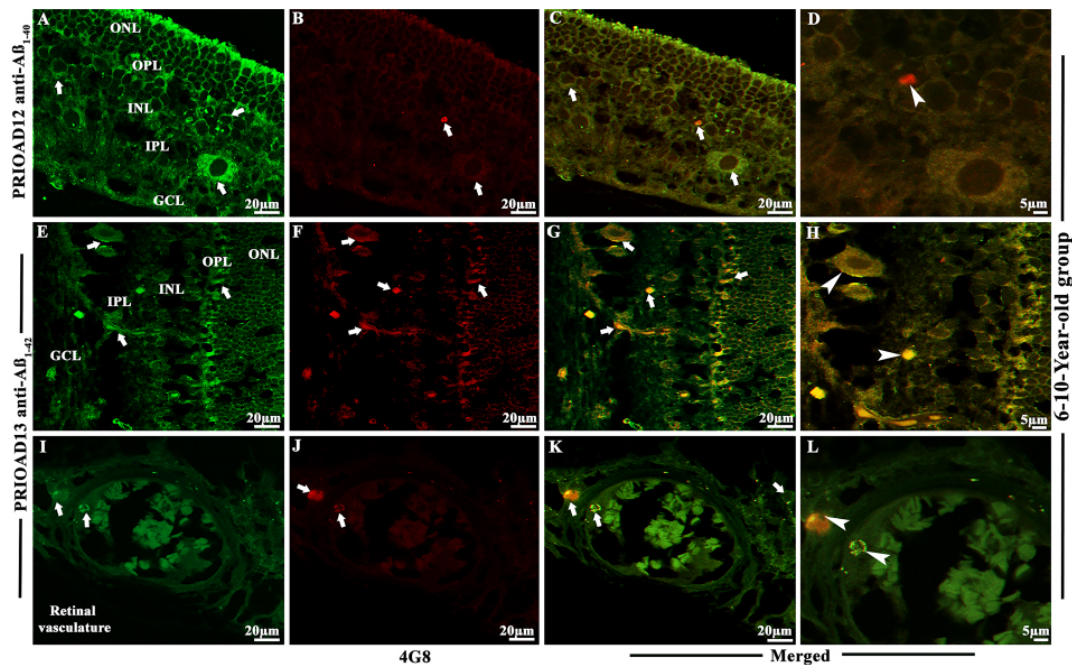


**Figure 3.** Immunofluorescence detection and co-localization of retinal amyloid-beta oligomers and amyloid-beta plaques in dogs of the 6-10-year-old group. Retinal co-staining with anti- $A\beta_{40}$  (PRIOAD 12) and anti- $A\beta_{42}$  (PRIOAD 13) camelid-derived single domain antibody (green) and 4G8 antibody (red) of a 9-year-old Cocker spaniel dog (A-L). (A) A large number of  $A\beta_{40}$  and (B)  $A\beta_{42}$  oligomers were found in the GCL, INL, and ONL (white arrows, 40 $\times$ ). (C) Detection of  $A\beta_{42}$  oligomers in the vasculature. 4G8 positive  $A\beta$  plaque-like deposits were observed in the (D and E) GCL, IPL, INL, and OPL of the retina (white arrows, 40 $\times$ ). Widespread co-localization was observed in the (G and H) retinal layers (white arrows, 40 $\times$ ). Co-localization of 4G8 positive  $A\beta$  plaque with (J)  $A\beta_{40}$  and (K)  $A\beta_{42}$  depositions (white arrowhead) showed with higher magnification (100 $\times$ ) in the GCL and INL of the same 9-year-old Cocker spaniel dog retinal section. (C)  $A\beta$  oligomers and (F) 4G8 positive  $A\beta$  plaques were observed in the retinal vasculature (white arrows). (I and L) Co-localization of  $A\beta$  oligomers and 4G8 positive  $A\beta$  plaques were exhibited with 40 $\times$  and with higher 100 $\times$  magnification in the retinal vessel wall, respectively (white arrowhead). The photomicrograph was derived from the peripheral region of the retina - away from the optic disc. Representative of 10 dogs examined from middle age group (6-10 years). GCL: Ganglion cell layer; IPL: inner plexiform layer; INL: inner nuclear layer; OPL: outer plexiform layer; ONL: outer nuclear layer.

thirty dogs presented with eye neoplasms, including two in the young age group, seven in the middle age group, and nine in the old age group [Table 2]. There was no clear relation between neoplasms and the intensity of  $A\beta$  or p-Tau [Table 2]. Interestingly, eye inflammation (proptosis/ phthisis bulbi in young dogs and conjunctivitis in a middle-aged dog) corresponded to  $A\beta_{40}$  and  $A\beta_{42}$  oligomers intensity that ranged from "moderate" to "strong" [Table 2]. Finally, a case of pre-glaucoma in the middle age group and a case of glaucoma in the old age group also matched well with  $A\beta_{40}$  and  $A\beta_{42}$  oligomers as well as  $A\beta_p$  intensity. Overall, this analysis appears to indicate that no direct influence of pre-existing eye disorders on  $A\beta$  and p-Tau intensity exists; however, the small size of the cohorts used in this study did not allow to reach a substantive conclusion, and studies with much larger cohorts are needed.

## DISCUSSION

Eye imaging can provide an opportunity to develop an easily accessible and point-of-care routine diagnostic testing to help predict MCI/AD early<sup>[66,67]</sup>. A study by Ko and colleagues examined the retinal NFL thickness and cognitive status of individuals aged 40 to 69 years over three years<sup>[68]</sup>. The authors found that individuals with thinner NFL showed a higher incidence of reduced cognition.

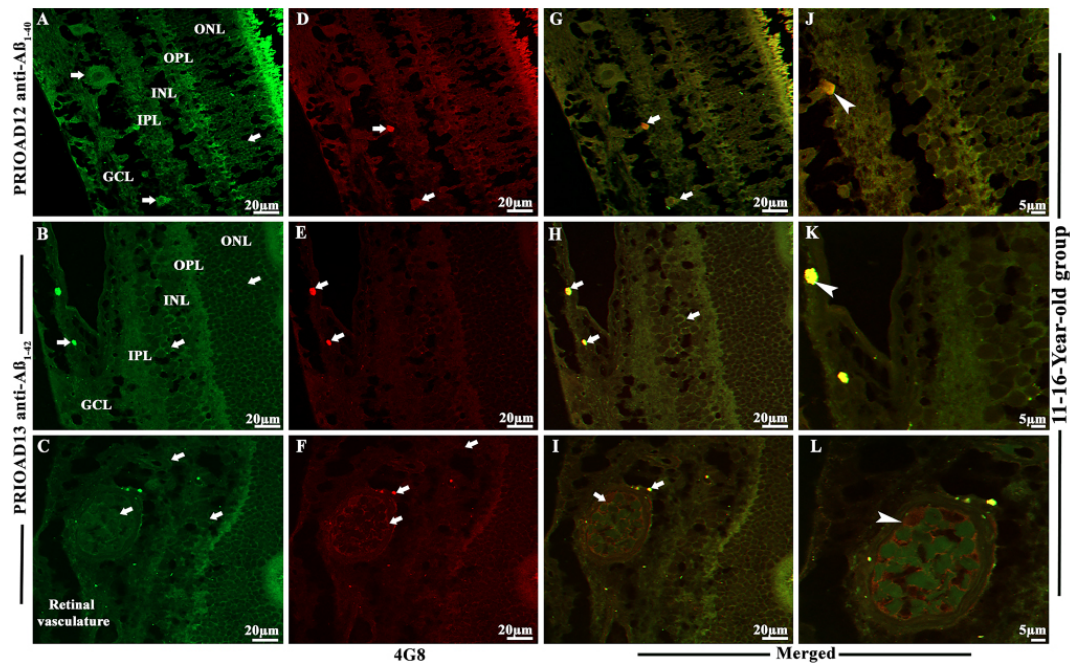


**Figure 4.** Immunofluorescence co-localization of retinal amyloid-beta oligomers and amyloid-beta plaques in dogs of 11-16-year-old group. Retinal co-staining with anti- $A\beta_{40}$  (PRIOAD 12) and anti- $A\beta_{42}$  (PRIOAD 13) camelid-derived single domain antibody (green) and 4G8 antibody (red) of a 12-year-old German shepherd dog (A-L). A large number of (A)  $A\beta_{40}$  and (B)  $A\beta_{42}$  oligomers were found in the GCL, INL, and ONL (white arrows, 40 $\times$ ). 4G8 positive  $A\beta$  plaque-like deposits were observed in the (D and E) GCL of the retina (white arrows, 40 $\times$ ). Widespread co-localization was observed in the (G and H) retinal layers (white arrows, 40 $\times$ ). Co-localization of 4G8 positive  $A\beta$  plaque with (J)  $A\beta_{40}$  and (K)  $A\beta_{42}$  depositions (white arrowhead) showed with higher magnification (100 $\times$ ) in the GCL of the same 12-year-old German shepherd dog retinal section. (C)  $A\beta$  oligomers and (F) 4G8 positive  $A\beta$  plaques were observed in the retinal vasculature (white arrows). (I and L) Co-localization of  $A\beta$  oligomers and 4G8 positive  $A\beta$  plaques were exhibited with 40 $\times$  and also with higher 100 $\times$  magnification in the retinal vessel wall, respectively (white arrowhead). The photomicrograph was derived from the peripheral region of the retina - away from the optic disc. Representative of 10 dogs examined from elder age group (11-16 years). GCL: ganglion cell layer; INL: inner nuclear layer; ONL: outer nuclear layer.

Despite the validation of the dog as a robust translational model for AD<sup>[24,30,69]</sup>, only very limited studies investigated AD-related changes in the young and neurologically intact dogs. One study by Stylianaki and colleagues confirmed a similar pattern to that of humans; 61 dogs were subdivided into young (0-4 years old), middle-aged (4-8 years old), aged cognitively normal (8-20 years old), and aged cognitively impaired (8-17 years-old)<sup>[70]</sup>. The authors found that young dogs displayed the highest levels of total plasma  $A\beta_{42}$  and  $A\beta_{42}/A\beta_{40}$  ratio and the middle-aged dogs had the highest cerebrospinal fluid  $A\beta_{40}$  and  $A\beta_{42}$  when compared to neurologically intact aged dogs. Our first step was to investigate the distribution and morphological appearance of both  $A\beta_{40}$  and  $A\beta_{42}$  oligomers representing the canine lifetime, in the retinal layers of these neurologically intact 30 dogs. Previous studies have shown that A11 anti-oligomer antibody binds to different epitopes of the  $A\beta$  but also reacts with oligomeric aggregates of other proteins independent of their primary sequences. Of note, A11 cannot differentiate between  $A\beta_{40}$  and  $A\beta_{42}$ . In contrast, PRIOAD12 and PRIOAD13 nanobodies bind to  $A\beta_{40}$  and  $A\beta_{42}$ , respectively. Previous studies reported an inverse interrelationship between neurotoxicity and the size of  $A\beta$ , where the toxic effect of  $A\beta$  was shown to decrease with increased size. The general molecular weight of  $A\beta$  was found to range between 10-100 kDa in AD brain and included dimers to dodecamer<sup>[71]</sup>. A study by Lambert and colleagues first describes the cytotoxic effect of the small diffusible  $A\beta$  on the hippocampal neurons<sup>[72]</sup>. The small  $A\beta$  referred to as  $A\beta$ -derived diffusible ligands toxicity was tested in organotypic mouse brain slice cultures. The authors found that 17 and 22 kDa small oligomers killed hippocampal neurons at nanomolar concentration<sup>[72]</sup>. In addition, a study by Cizas and colleagues confirmed that oligomers larger than 30 kDa have a less toxic effect on the

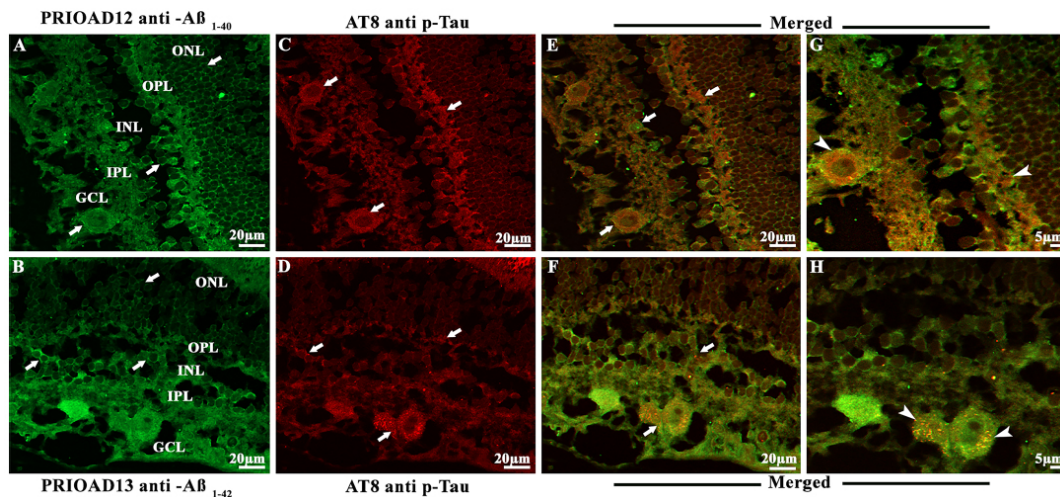


**Figure 5.** Immunofluorescence co-localization of retinal amyloid-beta oligomers and hyperphosphorylated tau in dogs of 11-16-year-old group. Retinal co-staining with anti-A $\beta_{40}$  (PRIOAD 12) and anti-A $\beta_{42}$  (PRIOAD 13) camelid-derived single domain antibody (green) and AT8 antibody (red) of a 12-year-old German shepherd dog. A large number of (A) A $\beta_{40}$  and (B) A $\beta_{42}$  oligomers were found in the GCL, INL, and ONL (white arrows, 40 $\times$ ). AT8 positive diffuse p-Tau-like deposits were observed in the (C and D) GCL, IPL, INL, and OPL of the retina (white arrows, 40 $\times$ ). Widespread co-localization was observed in the (E and F) retinal layers (white arrows, 40 $\times$ ). Co-localization of AT8 positive p-Tau with (G) A $\beta_{40}$  and (H) A $\beta_{42}$  depositions (white arrowhead) showed with higher magnification (100 $\times$ ) in the GCL and OPL of the same 12-year-old German shepherd dog retinal section. The photomicrograph was derived from the peripheral region of the retina - away from the optic disc. Representative of 10 dogs examined from elder age group ( $\geq 11$  years). GCL: Ganglion cell layer; IPL: inner plexiform layer; INL: inner nuclear layer; OPL: outer plexiform layer; ONL: outer nuclear layer.

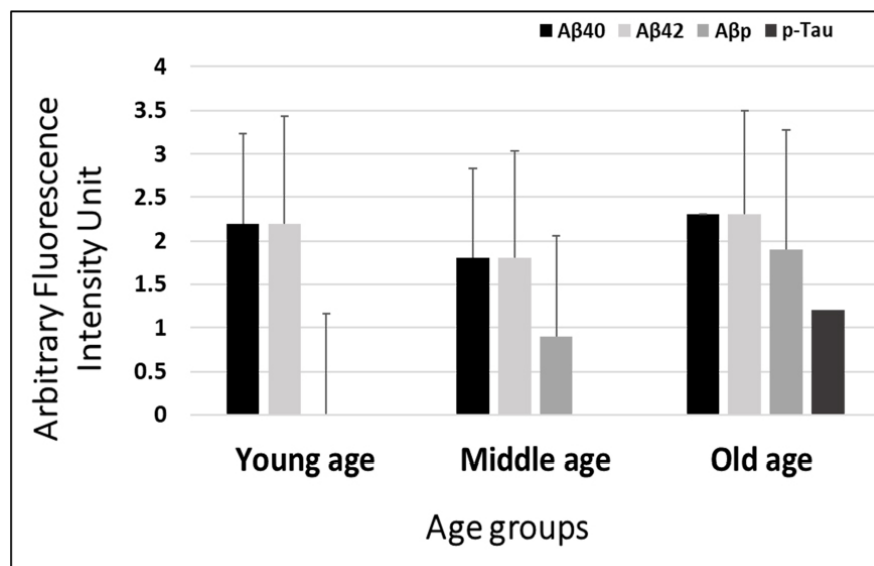


**Figure 6.** Semiquantitative analysis of A $\beta_{40}$  and A $\beta_{42}$  oligomers, A $\beta$  plaques, and p-Tau in neurologically intact young (1-5-years), middle (6-10-years), and old (11-16-years) age groups of dogs. PRIOAD12 (A $\beta_{40}$  oligomers), PRIOAD13 (A $\beta_{42}$  oligomers), 4G8 (A $\beta_p$ ), and AT8 (p-Tau) fluorescence immunoreactivity and intensities were examined and quantified at 40 $\times$  magnification under the fluorescence microscope. Semiquantitative analyses were compared with the three different age groups. A large amount of A $\beta_{40}$  and A $\beta_{42}$  oligomers were found in young dogs, which decreased in middle age group, then finally, an upward trend was noticed in older dogs. In comparison, A $\beta_p$  were completely absent in young dogs, and then moderately found in middle, and large amounts in old age groups. Finally, p-Tau deposits were not found in young and middle age groups of dogs, whereas old dogs exhibited a considerable amount of p-Tau.

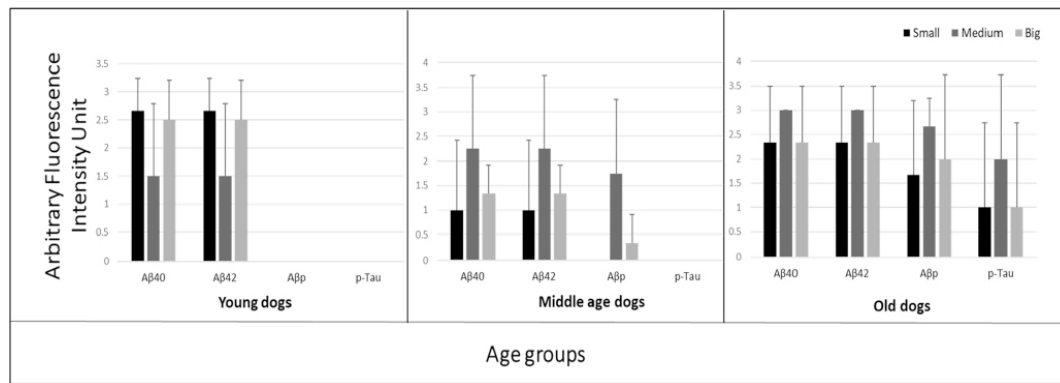


**Figure 7.** Influence of the size of dogs on the retinal deposition of amyloid-beta oligomers ( $A\beta_o$ ), plaques ( $A\beta_p$ ), and phosphorylated tau (p-Tau) in cognitively unimpaired young (1-5-years), middle (6-10-years) and old (11-16-years) age groups of dogs. PRIOAD12 ( $A\beta_{40}$  oligomers), PRIOAD13 ( $A\beta_{42}$  oligomers), 4G8 ( $A\beta_p$ ), and AT8 (p-Tau) fluorescence immunoreactivity and intensities were examined and quantified at 40 $\times$  magnification under the fluorescence microscope. In three different age groups, semiquantitative analyses were compared with the size of the dogs. In young dogs, a large number of oligomers were displayed by the small and big size dogs. The majority of medium-sized dogs displayed strong  $A\beta_o$  and  $A\beta_p$  staining intensity in the middle-aged dogs. Finally, among the different sizes of old dogs, medium-sized breeds displayed the highest amount of  $A\beta_o$ ,  $A\beta_p$ , and p-Tau staining intensity.

inhibition of long-term potentiation<sup>[73]</sup>. They also suggested the transition of sizes from small to large correlate with the high to a low toxic effect of  $A\beta_o$ <sup>[73]</sup>. A11 specifically binds to the prefibrillar oligomers. However, studies suggested that the specificity of A11 to AD-related oligomers might vary as it recognized prefibrillar oligomers from various proteins that share a common structure including  $\alpha$ -synuclein, islet amyloid polypeptide, polyglutamine (PolyQ), lysozyme, and prion peptide<sup>[36]</sup>. A study by Glabe and colleagues reported the ideal band size of prefibrillar oligomer-specific antibody A11 ranged from approximately tetrameric up to ~75 kDa<sup>[35]</sup>. In our study, we confirmed the presence of an A11-specific band at ~70kDa, confirming binding to prefibrillar oligomers in APP/PS1 mice. In comparison, camelid-derived single-domain nanobodies bind to ~15kDa band representing the small oligomers. In agreement with this current study, our previous report<sup>[55]</sup> also suggested that nanobodies were able to detect the toxic small diffusible oligomers specific to AD, whereas A11 binds to the larger oligomers believed to be less toxic to the neurons.

Studies suggested that in the canine brain,  $A\beta_o$  may be the toxic species responsible for cognitive decline and can potentially be an early biomarker for the detection of CCD<sup>[23,74]</sup>. Naaman and colleagues recently reported that  $A\beta_{42}$  oligomers cause extensive retinal neurotoxicity in rats when compared to fibrillary  $A\beta_{40}$  and  $A\beta_{42}$ <sup>[75]</sup>. Our findings demonstrated extensive deposition of  $A\beta_{40}$  and  $A\beta_{42}$  oligomers in the retinal layers, including GCL, INL, and ONL in 26/30 in the young, middle, and old age groups, except for a 1.4-year-old male Siberian husky, a 7-year-old neutered male Hound mixed, an 8-year-old spayed female Bedlington terrier, and an 11-year-old neutered male mixed breed. Moreover, we did not notice any difference in the intensity of immunofluorescence (graded - to +++), the pattern of deposition, or morphology between  $A\beta_{40}$  and  $A\beta_{42}$  oligomers in all age groups. This presentation was unlikely influenced by the breed of the animals; for instance, out of three Siberian Huskies, one dog failed to display  $A\beta_{40}$  and  $A\beta_{42}$  oligomers accumulation. Remarkably, the younger age group, with an age range of 1-5 years, equivalent to humans aged 15-40 years according to the American Kennel Club<sup>[76]</sup>, has displayed extensive deposition of  $A\beta$  oligomers. Of interest, a 2013 brain study investigated the presence of three different types of  $A\beta$  oligomers, including  $A\beta$  trimers,  $A\beta^*56$ , and  $A\beta$  dimers, in 75 cognitively unimpaired individuals aged 1 to 96 years<sup>[14]</sup>. Young children and adolescents were positive for  $A\beta$  oligomers; the authors found an age-related accumulation of  $A\beta$  oligomers where the level of the amyloid- $\beta$  dimer was significantly higher in subjects in their 60s, and amyloid- $\beta$  trimer

in their 70s, whereas A $\beta$ \*56 level was significantly higher in individuals in their 40s. The investigators proposed that A $\beta$ o, specifically A $\beta$ \*56, might trigger the pathological cascade in asymptomatic AD, a phase that may be identifiable two decades before the clinical onset<sup>[14]</sup>.

Having found that the eyes of 26/30 dogs contained A $\beta$ <sub>40</sub> and A $\beta$ <sub>42</sub> oligomers, our next step was to demonstrate the presence/deposition of fibrillar A $\beta$  in the canine retina of this same cohort. We show that none of the young dogs displays 4G8-positive A $\beta$  fibrils and plaques (A $\beta$ p). However, A $\beta$ p were observed in some of the middle age group, where three dogs exhibited "low" staining intensity and two exhibited "strong" staining intensity in the GCL, IPL & INL. A $\beta$ p were also observed in the old age group, where five dogs showed "strong" signal intensity and two with "moderate" signal intensity in the GCL, IPL & INL. A pattern, not surprising, emerges; A $\beta$ <sub>40</sub> and A $\beta$ <sub>42</sub> oligomers are deposited in the retina following birth and subsequently, a fibrillar A $\beta$  configuration, aggregated as plaques follow. Several studies have demonstrated the presence of A $\beta$ p in the canine brain and suggested only a weak correlation with the severity of cognitive dysfunction<sup>[77,78]</sup>. Schütt *et al.* investigated this question in further depth by studying dogs at differing ages, specifically aged 9-15 years, including neurologically intact dogs and dogs with CCD, and compared their amyloid burden with that of young dogs aged less than 6 years<sup>[69]</sup>. The authors reported that the levels of A $\beta$  deposition strongly correlated with the age of the dog but not to their cognitive capacity. Asking the same questions regarding amyloid accretion in non-CNS neuronal populations, such as the retina, has not been investigated in the canine, but some recent reports confirmed their presence in the retina of AD<sup>[50,54,79]</sup>. In this study, we have demonstrated accumulation of retinal A $\beta$ p in the mature to an aged group of these 30 dogs which supports the hypothesis that A $\beta$ p might not influence the severity of cognitive deficits but can be a predictor of AD development<sup>[11,17]</sup>. Overall, our study revealed that the A $\beta$  deposition pattern in the retina was such that A $\beta$ o was observed in all age groups, whereas A $\beta$ p accumulation was restricted to the middle and more intensely the old age group of dogs, regardless of demographic criteria, breed and gender. Interestingly, co-accumulation of both A $\beta$ o and A $\beta$ p were apparent in some middle and old dogs. This is in agreement with our report this year, where 17-18 months old APP/PS1 mice showed high levels of oligomers deposits in the retinal layers that co-localized with A $\beta$ p<sup>[55]</sup>. Previous neuropathological studies in AD have shown that cerebral A $\beta$ o is usually present in early disease stages and is the most cytotoxic of A $\beta$  species, mostly responsible for neurotoxicity and synaptic dysfunction<sup>[34,80-83]</sup>, whereas extracellular A $\beta$ p is believed to accumulate at later ages and may act as a reservoir for A $\beta$ o<sup>[84]</sup>. Moreover, the involvement of A $\beta$ o in retinal degeneration in AD has also been reported<sup>[85-87]</sup>. In the study reported herein, we noticed widespread distribution of A $\beta$ o in the retinal layers of dogs of all age groups, indicating potential involvement in retinal degeneration, perhaps leading to vision impairment in some dogs<sup>[88,89]</sup>. Of importance, a previous study by Ozawa and colleagues that focused on web and paper-based surveys of dogs aged  $\geq 10$  years to identify physical disturbances related to CCD showed that more than 90% of dogs affected with CCD had vision impairment<sup>[90]</sup>. In addition to the neural retina, we observed A $\beta$  deposition s in the retinal microvasculature of young, middle, and old age groups, which might imitate CAA in AD<sup>[91-93]</sup>. Sharafi *et al.* suggested that retinal vasculature changes captured by hyperspectral imaging can differentiate cerebral amyloid status between cognitively impaired and unimpaired individuals<sup>[94]</sup>.

Central to AD pathogenesis is the intraneuronal deposition of hyperphosphorylated tau (p-Tau) in granular form and eventual organization as NFTs, one of the cardinal neuropathological hallmarks<sup>[3,4]</sup>. In dogs with CCD, p-Tau, unlike NFTs, has been identified in the brain, but until recently, only in some cases. We speculate that, unlike human AD, p-Tau is only evident in pretangle granular form in dogs due to their shorter lifespan (Tayebi & Habiba, unpublished observation). p-Tau neuropathology was shown to develop about a decade before the formation of A $\beta$ p in AD brains and was hypothesized to trigger AD<sup>[95,96]</sup>. However, A $\beta$ o accumulation was shown to precede and drive p-Tau accumulation and transneuronal spread across

synapses in the parietal cortex of AD<sup>[96]</sup>.

In the retina of human AD patients, p-Tau displayed a diffuse pattern in the plexiform layers in the absence of NFTs<sup>[54]</sup>. Schön and colleagues reported the presence of AT8-positive intracellular NFTs and diffuse p-Tau signals in the retina of 5/6 deceased AD patients<sup>[97]</sup>. In this study, we investigated the presence of p-Tau Ser202/Thr205 to confirm the presence of retinal p-Tau in dogs. We revealed diffuse p-Tau distribution in the OPL, INL, IPL, and GCL in 4/10 dogs of the old age group, including a spayed female German shepherd and a neutered male Husky aged 12 years old, a neutered male Shih Tzu aged 12.8 years old, and a neutered male Border collie aged 13 years old. The same dogs also showed the widespread distribution of A $\beta$ <sub>40</sub> and/or A $\beta$ <sub>42</sub> oligomers and 4G8-positive A $\beta$ . Similarly, in the brains of cognitively impaired, 14-17 years old dogs, Abey and colleagues have demonstrated the presence of p-Tau Ser202/Thr205 and p-Tau Ser396 in 1/6 and 6/6, respectively<sup>[40]</sup>. This pattern of deposition strongly supports a possible age-dependent progression as observed in AD mice models<sup>[49,55]</sup>. Previous studies have shown that breed variance does not determine the pathological outcome associated with CCD in aged dogs<sup>[98,99]</sup>. In agreement, our study did not reveal any breed-dependent pathological accumulation.

While previous studies have demonstrated the presence of A $\beta$  and p-Tau in the aged dog brain<sup>[30,43]</sup>, Pugleise *et al.* proposed that the acquisition of diffuse A $\beta$  and p-Tau are unrelated and independent events of aged dogs<sup>[42]</sup>. Whether these two “ingredients” of AD dementia or CCD are closely linked (co-localized or at least act in concert) is likely crucial. In AD, it was shown that p-Tau and A $\beta$  cause neuronal toxicity and may act synergistically to trigger synaptic dysfunction<sup>[36,37,100]</sup>. Manczak and colleagues showed that A $\beta$ <sub>40</sub> or A $\beta$ <sub>42</sub> oligomers co-localized with p-Tau in the brains of AD patients<sup>[101]</sup>. The authors also reported that the interaction between A $\beta$  and p-Tau became more prominent with disease progression and was more pronounced at Braak stage V and VI compared to Braak stage III and IV<sup>[102,103]</sup>. The evidence from this canine retina study would support an interaction: we also show that p-Tau co-localized with A $\beta$ <sub>40</sub> or A $\beta$ <sub>42</sub> oligomers in the OPL, INL, IPL, and GCL of the retina of 4/10 dogs in the eldest age group. A recent PET brain imaging study by Lockhart *et al.*, which demonstrated the presence of both A $\beta$  and Tau pathology in cognitively normal older adults, showed a significant spatial correlation with A $\beta$  and Tau deposition<sup>[104]</sup>. Thus co-localization, while evident, does not itself necessarily imply neuronal cytotoxicity.

Several studies in the field of AD research highlighted the importance of diagnostic and therapeutic interventions in the asymptomatic phase while the individuals are cognitively intact<sup>[14,105]</sup>. However, it is challenging to first identify and then track disease progression in humans without sensitive, specific, and cost-effective early diagnostic approaches and a lack of robust natural translational models. In that context, dogs have the potential to be an effective natural model for the study of aging and AD. They share the same environment as humans<sup>[106,107]</sup>; there exists the option of brain CT and MRI imaging and intracranial biopsy, ease of cognitive testing which helps reduce physiological stress, and finally, a short lifespan<sup>[108]</sup>. Canine ophthalmology is a well-established clinical and investigative discipline (inherited retinopathies, for example). The current study provides strong impetus to track how this seemingly common process evolves, with potential consequences for aging, neurodegenerative disease, and also vision.

Lateralization in retinal and cerebral A $\beta$  levels was previously investigated in an AD mouse model<sup>[109]</sup>. Some studies revealed left posterior brain-dominant lateralization in A $\beta$ <sub>42/40</sub>; however, no left or right brain hemisphere or retinal dominance lateralization was observed for A $\beta$ <sub>40</sub> and A $\beta$ <sub>42</sub>. Although our current study does not provide information about left versus right retinal accumulation of A $\beta$ , the significance of the lateralization in human Alzheimer's and CCD remains unknown. Moreover, previous reports have shown that A $\beta$  accumulation was more prominent in the far-peripheral and mid-peripheral of the superior

temporal quadrant than in the central retina in AD patients<sup>[50,79]</sup>; however, in our study, no notable differences in A $\beta$  and tau deposition have been observed in different parts of the retina.

The canine eye tissues used in this study had been surgically removed in the course of managing spontaneous disorders of the globe, eyelids, or structures within the orbit which necessitated enucleation. It could be asked whether any of these conditions played any part in A $\beta$  and/or p-Tau deposition in the retina. We think this unlikely, given the diverse clinical conditions involved, which ranged from developmental abnormalities, inflammatory conditions, and proptosis to various neoplasms of differing grades of the eye, while other cases were disorders arising in the conjunctiva or orbit. The span of ages in these dogs (from juvenile to quite aged) would further make this seem unlikely and some evidence of human retinal A $\beta$  and/or p-Tau exists, though such explorations are largely performed only at the end of life.

The study presented here offers valuable insights into the deposition patterns of amyloid beta (A $\beta$ ) and phosphorylated tau (p-Tau) in the canine retina. However, it is important to highlight that the sample size of dogs may limit the generalizability of our results. Additionally, the cross-sectional design of the study means we cannot establish temporal relationships between A $\beta$ /p-Tau deposition and cognitive decline. Longitudinal studies would provide a more comprehensive understanding of the progression of retinal pathology in correlation with cognitive status. Finally, it is important to recognize species differences, as dogs may not perfectly mirror human neurodegenerative processes. Therefore, caution is warranted when translating our findings into human clinical practice. Future research should explore whether ocular pathology itself contributes to retinal amyloidogenesis and tauopathy. Addressing these limitations through larger sample sizes, longitudinal designs, and careful consideration of confounding factors will strengthen the validity and clinical relevance of future investigations into retinal biomarkers for neurodegenerative diseases.

## DECLARATIONS

### Authors' contributions

Performed experiments and revised manuscript: Habiba U

Revised manuscript: Morley J, Krockenberger M

Was a major contributor in writing and revising the manuscript: Summers BA

Conceived and designed experiments and wrote manuscript: Tayebi M

All authors read and approved the final manuscript.

### Availability of data and materials

The data that support the findings of this study are available from authors.

### Financial support and sponsorship

None.

### Conflicts of interest

All authors declared that there are no conflicts of interest.

### Ethical approval and consent to participate

Sections of eyes used in this study were prepared from archived cases in the Comparative Ocular Pathology Laboratory of Wisconsin (COFLOW) at the Department of Pathobiological Sciences, School of Veterinary Medicine, University of Wisconsin, Madison. Such tissues, historically submitted for disease investigation purposes, are not subject to approval by institutional animal ethical regulations.

## Consent for publication

Not applicable.

## Copyright

© The Author(s) 2022.

## REFERENCES

1. Clark CM, Karlawish JHT. Alzheimer disease: current concepts and emerging diagnostic and therapeutic strategies. *Ann Intern Med* 2003;138:400-10. [DOI](#) [PubMed](#)
2. Mott RT, Hulette CM. Neuropathology of Alzheimer's disease. *Neuroimaging Clinics* 2005;15:755-65. [DOI](#) [PubMed](#)
3. Perl DP. Neuropathology of Alzheimer's disease. *Mt Sinai J Med* 2010;77:32-42. [DOI](#) [PubMed](#) [PMC](#)
4. Serrano-Pozo A, Frosch MP, Masliah E, Hyman BT. Neuropathological alterations in Alzheimer disease. *Cold Spring Harb Perspect Med* 2011;1:a006189. [DOI](#) [PubMed](#) [PMC](#)
5. Hardy J, Selkoe DJ. The amyloid hypothesis of Alzheimer's disease: progress and problems on the road to therapeutics. *Science* 2002;297:353-6. [DOI](#) [PubMed](#)
6. Jack CR Jr, Wiste HJ, Weigand SD, et al. Age, sex, and APOE ε4 effects on memory, brain structure, and β-amyloid across the adult life span. *JAMA Neurol* 2015;72:511-9. [DOI](#) [PubMed](#) [PMC](#)
7. Rentz DM, Locascio JJ, Becker JA, et al. Cognition, reserve, and amyloid deposition in normal aging. *Ann Neurol* 2010;67:353-64. [DOI](#) [PubMed](#) [PMC](#)
8. Rodrigue KM, Kennedy KM, Park DC. Beta-amyloid deposition and the aging brain. *Neuropsychol Rev* 2009;19:436-50. [DOI](#) [PubMed](#) [PMC](#)
9. Oh H, Mormino EC, Madison C, Hayenga A, Smiljic A, Jagust WJ. β-amyloid affects frontal and posterior brain networks in normal aging. *Neuroimage* 2011;54:1887-95. [DOI](#) [PubMed](#) [PMC](#)
10. Bourgeat P, Chételat G, Villemagne VL, et al; AIBL Research Group. Beta-amyloid burden in the temporal neocortex is related to hippocampal atrophy in elderly subjects without dementia. *Neurology* 2010;74:121-7. [DOI](#) [PubMed](#)
11. Rowe CC, Ellis KA, Rimajova M, et al. Amyloid imaging results from the Australian Imaging, Biomarkers and Lifestyle (AIBL) study of aging. *Neurobiol Aging* 2010;31:1275-83. [DOI](#) [PubMed](#)
12. Petersen RC, Aisen P, Boeve BF, et al. Mild cognitive impairment due to Alzheimer disease in the community. *Ann Neurol* 2013;74:199-208. [DOI](#) [PubMed](#) [PMC](#)
13. Erten-Lyons D, Woltjer RL, Dodge H, et al. Factors associated with resistance to dementia despite high Alzheimer disease pathology. *Neurology* 2009;72:354-60. [DOI](#) [PubMed](#) [PMC](#)
14. Lesné SE, Sherman MA, Grant M, et al. Brain amyloid-β oligomers in ageing and Alzheimer's disease. *Brain* 2013;136:1383-98. [DOI](#) [PubMed](#) [PMC](#)
15. Bischof GN, Rodrigue KM, Kennedy KM, Devous MD Sr, Park DC. Amyloid deposition in younger adults is linked to episodic memory performance. *Neurology* 2016;87:2562-6. [DOI](#) [PubMed](#) [PMC](#)
16. Hanseeuw BJ, Betensky RA, Jacobs HIL, et al. Association of amyloid and tau with cognition in preclinical Alzheimer disease: a longitudinal study. *JAMA Neurol* 2019;76:915-24. [DOI](#) [PubMed](#) [PMC](#)
17. Rowe CC, Bourgeat P, Ellis KA, et al. Predicting Alzheimer disease with β-amyloid imaging: results from the Australian imaging, biomarkers, and lifestyle study of ageing. *Ann Neurol* 2013;74:905-13. [DOI](#) [PubMed](#)
18. Drummond E, Wisniewski T. Alzheimer's disease: experimental models and reality. *Acta Neuropathol* 2017;133:155-75. [DOI](#) [PubMed](#) [PMC](#)
19. Kitazawa M, Medeiros R, Laferla FM. Transgenic mouse models of Alzheimer disease: developing a better model as a tool for therapeutic interventions. *Curr Pharm Des* 2012;18:1131-47. [DOI](#) [PubMed](#) [PMC](#)
20. Cummings BJ, Head E, Ruehl W, Milgram NW, Cotman CW. The canine as an animal model of human aging and dementia. *Neurobiology of Aging* 1996;17:259-68. [DOI](#) [PubMed](#)
21. Head E, McCleary R, Hahn FF, Milgram NW, Cotman CW. Region-specific age at onset of β-amyloid in dogs. *Neurobiol Aging* 2000;21:89-96. [DOI](#) [PubMed](#)
22. Pugliese M, Gangitano C, Ceccariglia S, et al. Canine cognitive dysfunction and the cerebellum: acetylcholinesterase reduction, neuronal and glial changes. *Brain Res* 2007;1139:85-94. [DOI](#) [PubMed](#)
23. Head E, Pop V, Sarsoza F, et al. Amyloid-beta peptide and oligomers in the brain and cerebrospinal fluid of aged canines. *J Alzheimers Dis* 2010;20:637-46. [DOI](#) [PubMed](#) [PMC](#)
24. Youssef SA, Capucchio MT, Rofina JE, et al. Pathology of the aging brain in domestic and laboratory animals, and animal models of human neurodegenerative diseases. *Vet Pathol* 2016;53:327-48. [DOI](#) [PubMed](#)
25. Cummings BJ, Head E, Afagh AJ, Milgram NW, Cotman CW. Beta-amyloid accumulation correlates with cognitive dysfunction in the aged canine. *Neurobiol Learn Mem* 1996;66:11-23. [DOI](#) [PubMed](#)
26. Adams B, Chan A, Callahan H, Milgram NW. The canine as a model of human cognitive aging: recent developments. *Prog Neuropsychopharmacol Biol Psychiatry* 2000;24:675-92. [DOI](#) [PubMed](#)

27. Head E. A canine model of human aging and Alzheimer's disease. *Biochim Biophys Acta* 2013;1832:1384-9. DOI PubMed PMC
28. Rofina JE, van Ederen AM, Toussaint MJ, et al. Cognitive disturbances in old dogs suffering from the canine counterpart of Alzheimer's disease. *Brain Res* 2006;1069:216-26. DOI PubMed
29. Chow VW, Mattson MP, Wong PC, Gleichmann M. An overview of APP processing enzymes and products. *Neuromolecular Med* 2010;12:1-12. DOI PubMed PMC
30. Yu CH, Song GS, Yhee JY, et al. Histopathological and immunohistochemical comparison of the brain of human patients with Alzheimer's disease and the brain of aged dogs with cognitive dysfunction. *J Comp Pathol* 2011;145:45-58. DOI PubMed
31. Broersen K, Rousseau F, Schymkowitz J. The culprit behind amyloid beta peptide related neurotoxicity in Alzheimer's disease: oligomer size or conformation? *Alzheimers Res Ther* 2010;2:12. DOI PubMed PMC
32. Goure WF, Krafft GA, Jerecic J, Hefti F. Targeting the proper amyloid-beta neuronal toxins: a path forward for Alzheimer's disease immunotherapeutics. *Alzheimers Res Ther* 2014;6:42. DOI PubMed PMC
33. Morgado I, Fändrich M. Assembly of Alzheimer's A $\beta$  peptide into nanostructured amyloid fibrils. *Current opinion in colloid & interface science* 2011;16:508-14. DOI
34. Sengupta U, Nilson AN, Kaye R. The role of amyloid- $\beta$  oligomers in toxicity, propagation, and immunotherapy. *EBioMedicine* 2016;6:42-9. DOI PubMed PMC
35. Glabe CG. Structural classification of toxic amyloid oligomers. *J Biol Chem* 2008;283:29639-43. DOI PubMed PMC
36. Kaye R, Head E, Thompson JL, et al. Common structure of soluble amyloid oligomers implies common mechanism of pathogenesis. *Science* 2003;300:486-9. DOI PubMed
37. Haass C, Selkoe DJ. Soluble protein oligomers in neurodegeneration: lessons from the Alzheimer's amyloid beta-peptide. *Nat Rev Mol Cell Biol* 2007;8:101-12. DOI PubMed
38. Benilova I, Karran E, De Strooper B. The toxic A $\beta$  oligomer and Alzheimer's disease: an emperor in need of clothes. *Nat Neurosci* 2012;15:349-57. DOI PubMed
39. Zhao LN, Long HW, Mu Y, Chew LY. The toxicity of amyloid  $\beta$  oligomers. *International journal of molecular sciences* 2012;13:7303-27. DOI
40. Abey A, Davies D, Goldsbury C, Buckland M, Valenzuela M, Duncan T. Distribution of tau hyperphosphorylation in canine dementia resembles early Alzheimer's disease and other tauopathies. *Brain Pathol* 2021;31:144-62. DOI PubMed PMC
41. Papaioannou N, Tooten PC, van Ederen AM, et al. Immunohistochemical investigation of the brain of aged dogs. I. Detection of neurofibrillary tangles and of 4-hydroxynonenal protein, an oxidative damage product, in senile plaques. *Amyloid* 2001;8:11-21. DOI PubMed
42. Pugliese M, Mascort J, Mahy N, Ferrer I. Diffuse beta-amyloid plaques and hyperphosphorylated tau are unrelated processes in aged dogs with behavioral deficits. *Acta Neuropathol* 2006;112:175-83. DOI PubMed
43. Schmidt F, Boltze J, Jäger C, et al. Detection and quantification of  $\beta$ -amyloid, pyroglutamyl A $\beta$ , and tau in aged canines. *J Neuropathol Exp Neurol* 2015;74:912-23. DOI PubMed
44. Wegiel J, Wisniewski HM, Soltysiak Z. Region- and cell-type-specific pattern of tau phosphorylation in dog brain. *Brain Research* 1998;802:259-66. DOI PubMed
45. Armstrong RA. Alzheimer's disease and the eye. *Journal of Optometry* 2009;2:103-11. Available from: <https://doi.org/10.3921/joptom.2009.103>.
46. Santos CY, Johnson LN, Sinoff SE, Festa EK, Heindel WC, Snyder PJ. Change in retinal structural anatomy during the preclinical stage of Alzheimer's disease. *Alzheimers Dement (Amst)* 2018;10:196-209. DOI PubMed PMC
47. Marquié M, Castilla-Martí M, Valero S, et al. Visual impairment in aging and cognitive decline: experience in a Memory Clinic. *Sci Rep* 2019;9:8698. DOI PubMed PMC
48. Lee ATC, Richards M, Chan WC, Chiu HFK, Lee RSY, Lam LCW. Higher dementia incidence in older adults with poor visual acuity. *J Gerontol A Biol Sci Med Sci* 2020;75:2162-8. DOI PubMed PMC
49. Habiba U, Merlin S, Lim JKH, et al. Age-specific retinal and cerebral immunodetection of amyloid- $\beta$  plaques and oligomers in a rodent model of Alzheimer's disease. *J Alzheimers Dis* 2020;76:1135-50. DOI PubMed
50. Lee S, Jiang K, McIlmoyle B, et al. Amyloid Beta immunoreactivity in the retinal ganglion cell layer of the Alzheimer's eye. *Front Neurosci* 2020;14:758. DOI PubMed PMC
51. Koronyo-Hamaoui M, Koronyo Y, Ljubimov AV, et al. Identification of amyloid plaques in retinas from Alzheimer's patients and noninvasive in vivo optical imaging of retinal plaques in a mouse model. *Neuroimage* 2011;54 Suppl 1:S204-17. DOI PubMed PMC
52. Tsai Y, Lu B, Ljubimov AV, et al. Ocular changes in TgF344-AD rat model of Alzheimer's disease. *Invest Ophthalmol Vis Sci* 2014;55:523-34. DOI PubMed PMC
53. Jentsch S, Schweitzer D, Schmidtke KU, et al. Retinal fluorescence lifetime imaging ophthalmoscopy measures depend on the severity of Alzheimer's disease. *Acta Ophthalmol* 2015;93:e241-7. DOI PubMed
54. den Haan J, Morrema THJ, Verbraak FD, et al. Amyloid-beta and phosphorylated tau in post-mortem Alzheimer's disease retinas. *Acta Neuropathol Commun* 2018;6:147. DOI PubMed PMC
55. Habiba U, Descallar J, Kreilaus F, et al. Detection of retinal and blood A $\beta$  oligomers with nanobodies. *Alzheimers Dement (Amst)* 2021;13:e12193. DOI PubMed PMC
56. Yi J, Chen B, Yao X, Lei Y, Ou F, Huang F. Upregulation of the lncRNA MEG3 improves cognitive impairment, alleviates neuronal

- damage, and inhibits activation of astrocytes in hippocampus tissues in Alzheimer's disease through inactivating the PI3K/Akt signaling pathway. *J Cell Biochem* 2019;120:18053-65. DOI PubMed
57. David MA, Jones DR, Tayebi M. Potential candidate camelid antibodies for the treatment of protein-misfolding diseases. *J Neuroimmunol* 2014;272:76-85. DOI PubMed
  58. van Eersel J, Stevens CH, Przybyla M, et al. Early-onset axonal pathology in a novel P301S-Tau transgenic mouse model of frontotemporal lobar degeneration. *Neuropathol Appl Neurobiol* 2015;41:906-25. DOI PubMed
  59. Radde R, Bolmont T, Kaeser SA, et al. Abeta42-driven cerebral amyloidosis in transgenic mice reveals early and robust pathology. *EMBO Rep* 2006;7:940-6. DOI PubMed PMC
  60. Nakayama H, Uchida K, Doi K. A comparative study of age-related brain pathology - are neurodegenerative diseases present in nonhuman animals? *Med Hypotheses* 2004;63:198-202. DOI PubMed
  61. Cummings BJ, Pike CJ, Shankle R, Cotman CW.  $\beta$ -amyloid deposition and other measures of neuropathology predict cognitive status in Alzheimer's disease. *Neurobiology of Aging* 1996;17:921-33. DOI PubMed
  62. Breydo L, Uversky VN. Structural, morphological, and functional diversity of amyloid oligomers. *FEBS Lett* 2015;589:2640-8. DOI PubMed
  63. Silva EG, Dubielzig R, Zarfoss MK, Anibal A. Distinctive histopathologic features of canine optic nerve hypoplasia and aplasia: a retrospective review of 13 cases. *Vet Ophthalmol* 2008;11:23-9. DOI PubMed
  64. Rüttimann G, Daicker B. Complex colobomas in the anterior eye segment in a beagle hound. *Zentralbl Veterinarmed A* 1982;29:528-37. PubMed
  65. Williams DL. A comparative approach to anterior segment dysgenesis. *Eye (Lond)* 1993;7:607-16. DOI PubMed
  66. Casaletto KB, Ward ME, Baker NS, et al. Retinal thinning is uniquely associated with medial temporal lobe atrophy in neurologically normal older adults. *Neurobiol Aging* 2017;51:141-7. DOI PubMed PMC
  67. Alonso-Caneiro D, Read SA, Collins MJ. Automatic segmentation of choroidal thickness in optical coherence tomography. *Biomed Opt Express* 2013;4:2795-812. DOI PubMed PMC
  68. Ko F, Muthy ZA, Gallacher J, et al; UK Biobank Eye & Vision Consortium. Association of retinal nerve fiber layer thinning with current and future cognitive decline: a study using optical coherence tomography. *JAMA Neurol* 2018;75:1198-205. DOI PubMed PMC
  69. Schütt T, Helboe L, Pedersen LØ, Waldemar G, Berendt M, Pedersen JT. Dogs with cognitive dysfunction as a spontaneous model for early Alzheimer's disease: a translational study of neuropathological and inflammatory markers. *J Alzheimers Dis* 2016;52:433-49. DOI PubMed
  70. Stylianaki I, Polizopoulou ZS, Theodoridis A, Koutouzidou G, Baka R, Papaioannou NG. Amyloid-beta plasma and cerebrospinal fluid biomarkers in aged dogs with cognitive dysfunction syndrome. *J Vet Intern Med* 2020;34:1532-40. DOI PubMed PMC
  71. Kuo YM, Emmerling MR, Vigo-Pelfrey C, et al. Water-soluble abeta (N-40, N-42) oligomers in normal and Alzheimer disease brains. *J Biol Chem* 1996;271:4077-81. DOI PubMed
  72. Lambert MP, Barlow AK, Chromy BA, et al. Diffusible, nonfibrillar ligands derived from Abeta1-42 are potent central nervous system neurotoxins. *Proc Natl Acad Sci U S A* 1998;95:6448-53. DOI PubMed PMC
  73. Cizas P, Budvytyte R, Morkuniene R, et al. Size-dependent neurotoxicity of beta-amyloid oligomers. *Arch Biochem Biophys* 2010;496:84-92. DOI PubMed PMC
  74. Rusbridge C, Salguero FJ, David MA, et al. An aged canid with behavioral deficits exhibits blood and cerebrospinal fluid amyloid beta oligomers. *Front Aging Neurosci* 2018;10:7. DOI PubMed PMC
  75. Naaman E, Ya'ari S, Itzkovich C, et al. The retinal toxicity profile towards assemblies of Amyloid- $\beta$  indicate the predominant pathophysiological activity of oligomeric species. *Sci Rep* 2020;10:20954. DOI PubMed PMC
  76. American Kennel Club. Dog years to human years 2018, January 02. Available from: <https://www.akcpetinsurance.com/blog/year-of-the-dog> [Last accessed on 23 May 2022].
  77. Ozawa M, Chambers JK, Uchida K, Nakayama H. The relation between canine cognitive dysfunction and age-related brain lesions. *J Vet Med Sci* 2016;78:997-1006. DOI PubMed PMC
  78. Kiatipattanasakul W, Nakamura S, Hossain MM, et al. Apoptosis in the aged dog brain. *Acta Neuropathol* 1996;92:242-8. DOI PubMed
  79. Koronyo Y, Biggs D, Barron E, et al. Retinal amyloid pathology and proof-of-concept imaging trial in Alzheimer's disease. *JCI Insight* 2017;2:93621. DOI PubMed PMC
  80. El-Agnaf OM, Salem SA, Paleologou KE, et al. Detection of oligomeric forms of alpha-synuclein protein in human plasma as a potential biomarker for Parkinson's disease. *FASEB J* 2006;20:419-25. DOI PubMed
  81. El-agnaf OM, Walsh DM, Allsop D. Soluble oligomers for the diagnosis of neurodegenerative diseases. *The Lancet Neurology* 2003;2:461-2. DOI PubMed
  82. Mucke L, Selkoe DJ. Neurotoxicity of amyloid  $\beta$ -protein: synaptic and network dysfunction. *Cold Spring Harb Perspect Med* 2012;2:a006338. DOI PubMed PMC
  83. Kim HJ, Chae SC, Lee DK, et al. Selective neuronal degeneration induced by soluble oligomeric amyloid beta protein. *FASEB J* 2003;17:118-20. DOI PubMed
  84. Mclean CA, Cherny RA, Fraser FW, et al. Soluble pool of A $\beta$ ? *Ann Neurol* 1999;46:860-6. DOI PubMed
  85. Lynn SA, Johnston DA, Scott JA, et al. Oligomeric A $\beta$ <sub>1-42</sub> induces an AMD-like phenotype and accumulates in lysosomes to impair

- RPE function. *Cells* 2021;10:413. DOI PubMed PMC
86. Ratnayaka JA, Serpell LC, Lotery AJ. Dementia of the eye: the role of amyloid beta in retinal degeneration. *Eye (Lond)* 2015;29:1013-26. DOI PubMed PMC
  87. Luihl V, Isas JM, Kaye R, Glabe CG, Langen R, Chen J. Drusen deposits associated with aging and age-related macular degeneration contain nonfibrillar amyloid oligomers. *J Clin Invest* 2006;116:378-85. DOI PubMed PMC
  88. Denenberg S, Liebel F, Rose J. Behavioural and medical differentials of cognitive decline and dementia in dogs and cats. In: Landsberg G, Madari A, Žilka N, editors. *Canine and feline dementia*. Cham: Springer International Publishing; 2017. p. 13-58. DOI
  89. Acland G, Aguirre G. Retinal degenerations in the dog: IV. Early retinal degeneration (erd) in Norwegian elkhounds. *Exp Eye Res* 1987;44:491-521. DOI PubMed
  90. Ozawa M, Inoue M, Uchida K, Chambers JK, Takeuchi Y, Nakayama H. Physical signs of canine cognitive dysfunction. *J Vet Med Sci* 2019;81:1829-34. DOI PubMed PMC
  91. Weber SA, Patel RK, Lutsep HL. Cerebral amyloid angiopathy: diagnosis and potential therapies. *Expert Rev Neurother* 2018;18:503-13. DOI PubMed
  92. Patton N, Aslam T, Macgillivray T, Pattie A, Deary IJ, Dhillon B. Retinal vascular image analysis as a potential screening tool for cerebrovascular disease: a rationale based on homology between cerebral and retinal microvasculatures. *J Anat* 2005;206:319-48. DOI PubMed PMC
  93. Shi H, Koronyo Y, Rentsendorj A, et al. Identification of early pericyte loss and vascular amyloidosis in Alzheimer's disease retina. *Acta Neuropathol* 2020;139:813-36. DOI PubMed PMC
  94. Sharafi SM, Sylvestre JP, Chevrefils C, et al. Vascular retinal biomarkers improves the detection of the likely cerebral amyloid status from hyperspectral retinal images. *Alzheimers Dement (N Y)* 2019;5:610-7. DOI PubMed PMC
  95. Arnsten AFT, Datta D, Del Tredici K, Braak H. Hypothesis: tau pathology is an initiating factor in sporadic Alzheimer's disease. *Alzheimers Dement* 2021;17:115-24. DOI PubMed PMC
  96. Bilousova T, Miller CA, Poon WW, et al. Synaptic amyloid- $\beta$  oligomers precede p-Tau and differentiate high pathology control cases. *Am J Pathol* 2016;186:185-98. DOI PubMed PMC
  97. Schön C, Hoffmann NA, Ochs SM, et al. Long-term in vivo imaging of fibrillar tau in the retina of P301S transgenic mice. *PLoS One* 2012;7:e53547. DOI PubMed PMC
  98. Rofina J, van Andel I, van Ederen AM, Papaioannou N, Yamaguchi H, Gruys E. Canine counterpart of senile dementia of the Alzheimer type: amyloid plaques near capillaries but lack of spatial relationship with activated microglia and macrophages. *Amyloid* 2003;10:86-96. DOI PubMed
  99. Colle MA, Hauw JJ, Crespeau F, et al. Vascular and parenchymal abeta deposition in the aging dog: correlation with behavior. *Neurobiol Aging* 2000;21:695-704. DOI PubMed
  100. De Felice FG, Wu D, Lambert MP, et al. Alzheimer's disease-type neuronal tau hyperphosphorylation induced by A beta oligomers. *Neurobiol Aging* 2008;29:1334-47. DOI PubMed PMC
  101. Manczak M, Reddy PH. Abnormal interaction of oligomeric amyloid- $\beta$  with phosphorylated tau: implications to synaptic dysfunction and neuronal damage. *J Alzheimers Dis* 2013;36:285-95. DOI PubMed PMC
  102. Fein JA, Sokolow S, Miller CA, et al. Co-localization of amyloid beta and tau pathology in Alzheimer's disease synaptosomes. *Am J Pathol* 2008;172:1683-92. DOI PubMed PMC
  103. Takahashi RH, Capetillo-Zarate E, Lin MT, Milner TA, Gouras GK. Co-occurrence of Alzheimer's disease  $\beta$ -amyloid and  $\tau$  pathologies at synapses. *Neurobiol Aging* 2010;31:1145-52. DOI PubMed PMC
  104. Lockhart SN, Schöll M, Baker SL, et al. Amyloid and tau PET demonstrate region-specific associations in normal older people. *Neuroimage* 2017;150:191-9. DOI PubMed PMC
  105. Golde TE, Schneider LS, Koo EH. Anti- $\beta$  therapeutics in Alzheimer's disease: the need for a paradigm shift. *Neuron* 2011;69:203-13. DOI PubMed PMC
  106. Parker HG, Kim LV, Sutter NB, et al. Genetic structure of the purebred domestic dog. *Science* 2004;304:1160-4. DOI PubMed
  107. Davis PR, Head E. Prevention approaches in a preclinical canine model of Alzheimer's disease: benefits and challenges. *Front Pharmacol* 2014;5:47. DOI PubMed PMC
  108. Awano T, Johnson GS, Wade CM, et al. Genome-wide association analysis reveals a SOD1 mutation in canine degenerative myelopathy that resembles amyotrophic lateral sclerosis. *Proc Natl Acad Sci U S A* 2009;106:2794-9. DOI PubMed PMC
  109. Doustar J, Rentsendorj A, Torbati T, et al. Parallels between retinal and brain pathology and response to immunotherapy in old, late-stage Alzheimer's disease mouse models. *Ageing Cell* 2020;19:e13246. DOI PubMed PMC